DOI 10.5012/bkcs.2010.31.9.2588

Dissociation of the Phenylarsane Molecular Ion: A Theoretical Study

Sun Young Kim and Joong Chul Choe*

*Department of Chemistry, Dongguk University-Seoul, Seoul 100-715, Korea. *E-mail: jcchoe@dongguk.edu*
Received June 28, 2010, Accepted July 26, 2010

The potential energy surfaces (PESs) for the primary and secondary dissociations of the phenylarsane molecular ion (**1a**) were determined from the quantum chemical calculations using the G3(MP2)//B3LYP method. Several pathways for the loss of H• were determined and occurred though rearrangements as well as through direct bond cleavages. The kinetic analysis based on the PES for the primary dissociation showed that the loss of H_2 was more favored than the loss of H•, but the H• loss competed with the H_2 loss at high energies. The bicyclic isomer, 7-arsa-norcaradiene radical cation, was formed through the 1,2 shift of an α-H of **1a** and played an important role as an intermediate for the further rearrangements in the loss of H• and the losses of As• and AsH. The reaction pathways for the formation of the major products in the secondary dissociations of $[M-H]^+$ and $[M-H_2]^{+\bullet}$ were examined. The theoretical prediction explained the previous experimental results for the dissociation at high energies but not the dissociation at low energies.

Key Words: Potential energy surface, G3 calculation, RRKM calculation, Kinetics, Reaction pathway

Introduction

The dissociation of ionized polyatomic molecules has extensively been studied using various experimental and theoretical techniques.[1-13] Their reaction kinetics has often been understood by exploring the potential energy surfaces for the isomerizations and the dissociations. Ionized benzene derivatives are among the most interesting subjects to gas phase ion chemists. Recently, the isomerization and dissociation mechanisms of some ionized monosubstituted benzenes, $C_6H_5XH_n^{+\bullet}$ (X = C, N, O, Si, P, S, and As), have been proposed using quantum chemical calculations.[2-10] Both similarities and differences were found among their dissociation mechanisms. Ring expansion to seven-membered ring isomers is a common mechanism for theses molecular ions. This expansion is caused by the 1,2 shift of an α-H to the ipso carbon. After subsequent rearrangements, X is inserted into the benzene ring to form a seven-membered ring isomer. The roles of the seven-membered ring isomers vary for the molecular ions. In the dissociations of toluene and aniline molecular ions,[3,4] these isomers contribute to the loss of H•, whereas for the phenylphosphine and thiophenol molecular ions,[7,8] these isomers undergo a ring contraction to five-membered ring isomers followed by the elimination of HCP and C_2H_2, respectively. Loss of H_2 is an important dissociation channel in the dissociation of phenylsilane,[6] phenylphosphine,[7] or phenylarsane[9,10] molecular ions, but this loss is not observed in the toluene[3] or aniline[4] molecular ions. This difference is mainly due to the more extended and diffuse nature of the outermost p orbitals of Si, P, and As.

Recently, the dissociation of the phenylarsane molecular ion ($C_6H_5AsH_2^{+\bullet}$, **1a**) has been investigated by Letzel *et al*.[9,10] using experimental and theoretical methods. The mass spectra of phenylarsane and dideutero phenylarsane, $C_6H_5AsD_2$, were obtained together with the metastable ion dissociation (MID) and collision-induced dissociation (CID) spectra of $M^{+\bullet}$ and $[M-1]^+$.[9] The products of interest in the dissociation of **1a** were $C_6H_5AsH^+ + H•$, $C_6H_5As^{+\bullet} + H_2$, $C_6H_4As^+ + H_2 + H•$, $C_6H_7^+ +$ As•, $C_6H_6^{+\bullet}$ + AsH, and $C_6H_6^{+\bullet}$ + As• + H•. The experimental results showed that the reactivity was different at low and high energies. At low energies, the loss of H• was exclusive, while at high energies, the losses of H_2, AsH, and As• were more important. In the isotope labeling experiment, Letzel *et al*. observed the hydrogen scrambling before the dissociation at high energies but not at low energies. MP2[9] and density functional theory (DFT)[10] calculations were performed to obtain the potential energy surface (PES) for the dissociation, and the experimental results were explained. In this work, the PES for the main primary and secondary dissociations of **1a** were theoretically examined at a higher level than the level that was performed before. Based on the PES, the isomerization and dissociation kinetics were discussed.

Computational Methods

The molecular orbital calculations were performed using the Gaussian 09 suite of programs.[14] The geometry of the stationary points was optimized at the unrestricted B3LYP level of the DFT using the 6-31G(d) basis set. The transition state (TS) geometries that connected the stationary points were examined and checked by calculating the intrinsic reaction coordinates at the same level. For a better accuracy of the energies, the single point energy calculations were performed at the B3LYP/6-311+G (3df, 2p) level, and the Gaussian-3 (G3) MP2 theory calculations were carried out using the B3LYP density functional method (G3(MP2)//B3LYP).[15]

The RRKM expression was used to calculate the rate-energy dependence for the unimolecular reaction steps that were involved in the selected reaction pathways because the RRKM formula for the microcanonical ensemble was mathematically equivalent to the formula in the statistical quasi-equilibrium theory (QET) that was developed for the ionic dissociations:[16]

$$k(E) = \frac{\sigma N^{\ddagger}(E - E_0)}{h\rho(E)} \quad (1)$$

In this equation, E is the internal energy of the reactant, E_0 is the critical energy of the reaction, $N^{\ddagger}$ is the sum of the TS states, ρ is the density of the reactant states, σ is the reaction path degeneracy, and h is Planck's constant. $N^{\ddagger}$ and ρ were evaluated through a direct count of the states using the Beyer-Swinehart algorithm.[17] The vibrational frequencies that were obtained from the B3LYP/6-31G(d) calculations were scaled down by a factor of 0.9614.[18]

Results and Discussion

Primary dissociation. The following four primary dissociations of **1a** were investigated in this work.

$$C_6H_5AsH_2^{+\bullet} \rightarrow C_6H_6As^{+} + H\bullet \quad (2)$$

$$C_6H_5AsH_2^{+\bullet} \rightarrow C_6H_5As^{+\bullet} + H_2 \quad (3)$$

$$C_6H_5AsH_2^{+\bullet} \rightarrow C_6H_7^{+} + As\bullet \quad (4)$$

$$C_6H_5AsH_2^{+\bullet} \rightarrow C_6H_6^{+\bullet} + AsH \quad (5)$$

In the optimized structure of **1a**, the two H atoms of the AsH_2 group laid on the same side of the phenyl ring, which was similar to the phenylphosphine molecular ion[7] but different from the aniline molecular ion[4] with a planar structure (See Figure S1 in Supplementary Materials). The loss of H_2 occurred through the 1,1-H elimination via an ion-molecule complex **1b** to form the phenylarsinidene radical cation (**3a**) (See Figures S1 and S2 in Supplementary Materials). The PES for the primary dissociation that was obtained from the G3(MP2)//B3LYP calculations is shown in Figure 1. Notably, the calculated energy (71 kJ mol^{-1}) for the dissociation of the ion-molecule complex **1b** (**1b** → **3a** + H_2) was unusually large, even though it hardly affected the dissociation kinetics as discussed below. Likely, the energy for **3a** was largely overestimated in the G3(MP2)//B3LYP calculation. More reasonable energetic data were obtained at the B3LYP/6-311+G(3df,2p)//B3LYP/6-31G(d) level; 116, 79, and 86 kJ mol^{-1}, relative to **1a**, for **TS1a_1b**, **1b**, and **3a** + H_2, respectively. In this case, the dissociation energy was estimated to be 7 kJ mol^{-1}.

The phenylarsenium ion (**2a**) was formed through a direct As-H bond cleavage. Its TS could not be located, indicating that the dissociation occurred via a loose TS without a reverse barrier, as confirmed by scanning the PES. **2a** + H• was 57 kJ mol^{-1} less stable than **3a** + H_2. Several other pathways were determined for the loss of H• that occurred after the rearrangements. The *exo*-7-arsa-norcaradiene radical cation (*exo*-**1c**), which was more stable than **1a** by 36 kJ mol^{-1}, was formed as a result of the 1,2 shift of an H in the AsH_2 group. The *o*-isophenylarsane radical cation (**1d**) was formed through an additional 1,2-H shift. After the rotation of the AsH group to form another *o*-isophenylarsane radical cation, **1e**, its meta and para isomers (**1f**, **1g**, **1h**) were formed through consecutive H-ring walks. The corresponding TSs lied below the dissociation threshold. Then **2a** was formed through a direct C-H bond cleavage of the CH_2 group of each of these isophenylarsane isomeric ions. Alternatively, after the isomerization of *exo*-**1c** to the 7-arsa-norbornadiene radical

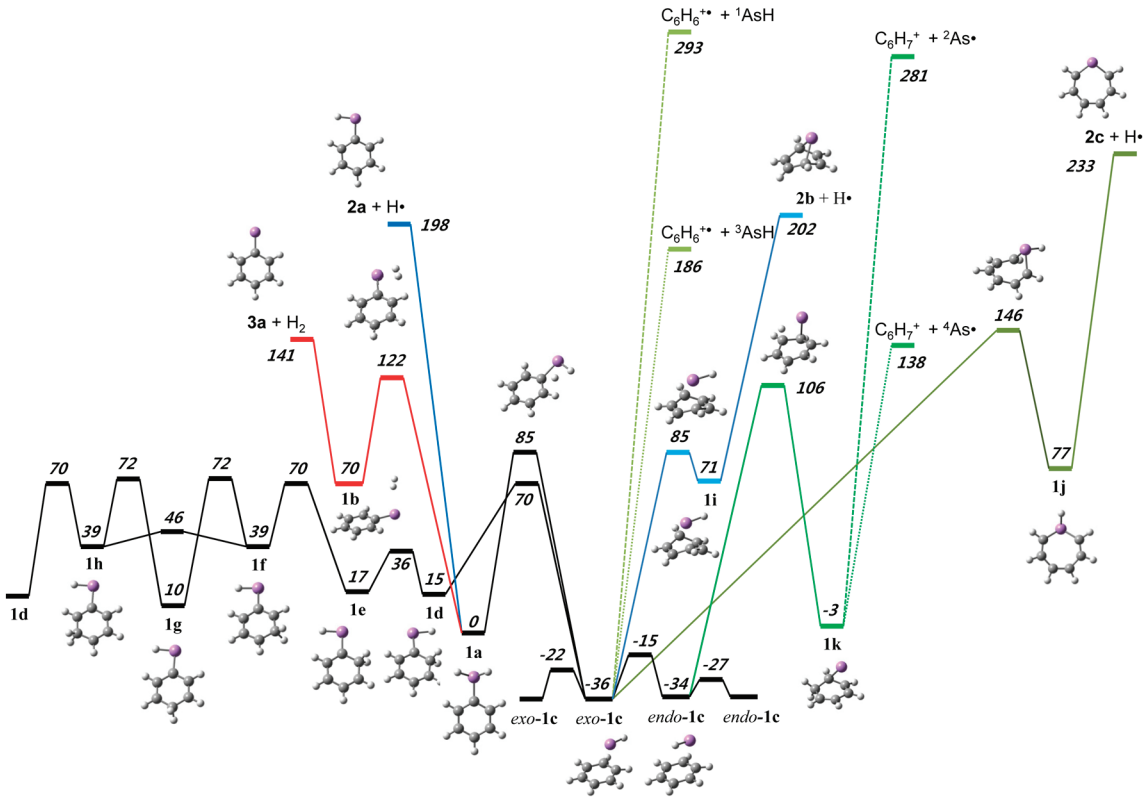

Figure 1. Potential energy diagram for the isomerization and the dissociation of **1a**, which was derived from the G3//B3LYP calculations. The energies are presented in kJ mol^{-1}. The calculated total energy of **1a** was −2466.693218 hartrees.

cation (**1i**), the 7-arsa-norbornadienyl cation (**2b**), which was less stable than **2a** by 4 kJ mol^{-1}, could be produced through the loss of H• without a reverse barrier. The loss of H• could occur via the seven-membered ring isomers. The 7-arsacycloheptatriene radical cation (**1j**) was formed through the insertion of the AsH group of *exo*-**1c** into the benzene ring, and then the arsatropylium ion (**2c**) was formed through the direct As-H bond cleavage. **2c** was less stable than **2a** by 35 kJ mol^{-1}. Therefore, thermodynamic predictions showed that the mixture of **2a** and **2b** was mainly produced through the loss of H• from **1a**.

Exo-**1c** was an important intermediate in the formation of the benzene and benzenium cations. The benzene radical cation was formed through the loss of AsH. The intersystem-crossing must occur from the doublet hypersurface in order to produce AsH in a triplet state (^{3}AsH), which was more stable than ^{1}AsH by 107 kJ mol^{-1}. The crossing point calculations were not performed because they were beyond the scope of this work. A similar loss of AsH occurred from *endo*-**1c** that was formed through the rotation of the AsH group of *exo*-**1c**. After the H-shift of the AsH group of *endo*-**1c** to the C-3 carbon, another bicyclic isomer, **1k**, was formed. The benzenium ion was formed through the loss of As• from **1k**. The As atom could be produced in a quartet state (^{4}As•) through the intersystem-crossing from the doublet hypersurface. Additionally, **2b** was produced from **1k** through loss of H•, but this mechanism was less important than the formation from *exo*-**1c** via **1i** because the first reaction occurred through a tight TS that was located 13 kJ mol^{-1} higher than the products, whereas the latter occurred through a loose TS.

The RRKM model calculation was carried out in order to gain an insight into the dissociation kinetics. The rate constants for the reactions **1a** → **1b**, **1a** → **2a** + H•, **1a** → *exo*-**1c**, and *exo*-**1c** → **1a** were calculated using the RRKM formalism in Equation 1. For the loss of H_2, the isomerization step **1a** → **1b** was the rate-limiting step because the reverse isomerization and the dissociation **1b** → **3a** + H_2 occurred very rapidly. Hence, the rate constant of the isomerization **1a** → **1b** was approximately equal to the dissociation **1a** → **3a** + H_2. The critical energies that were obtained from the G3(MP2)//B3LYP calculations were used in the RRKM calculations. In the rate calculation for the dissociation **1a** → **2a** + H•, one uncertainty occurred because the TS was not located. The activation entropy ($\Delta S^{\ddagger}$), which defined the degree of looseness of the TS,[16] was used in the calculation for this step. The RRKM rate constants generally do not depend on the individual vibrational frequencies but on the $\Delta S^{\ddagger}$.[16,19] As an approximation, the frequencies for the loose TS were adjusted so that $\Delta S^{\ddagger}$ was 7.0 eu (= 29 J mol^{-1} K^{-1}) at 1000 K, which was the middle value of the range (3.0 - 11 eu) for reactions that occured via loose TSs.[19] Before the isomerization of *exo*-**1c** to **1a**, the *exo*-to-*endo* isomerization proceeded very rapidly. Hence, the density of *endo*-**1c** was included as well as the density of *exo*-**1c** (as the denominator in Equation 1) in the rate calculation for *exo*-**1c** → **1a**. The reaction path degeneracy (σ) of 2 was used for all four reactions.

The resultant rate-energy dependences for the four reaction steps are shown in Figure 2. The results predicted that the isomerization of **1a** to *exo*-**1c** occurred more rapidly than the dissociations below 690 kJ mol^{-1}. Once *exo*-**1c** was formed, the isomerizations to *endo*-**1c** and the isophenylarsane radical cations easily occurred before dissociation. Both *exo*- and *endo*-**1c** also rapidly underwent a degenerate isomerization through an AsH ring walk. These isomerizations contributed to the H/D scrambling before the dissociation, which was observed in the CID of $C_6H_5AsD_2^{+\bullet}$.[9] The calculated rate-energy curves indicated that the loss of H_2 was predominant at low and moderate energies and the loss of H• became important as the energy increased. Before the dissociation, the isomerizations to *exo*- and *endo*-**1c**, which were more stable than **1a**, played a role as the kinetic trap. Namely, the dissociation rate constants were smaller than the calculated values as shown in Figure 2. The loss of H• from the isophenylarsane radical cations (**1d** - **1h**), as well as the direct loss of H• from **1a**, contributed to the formation of **2a**. On the other hand, only two pathways were determined for the formation of **2b** through the loss of H•. Therefore, the formation of **2a** through the loss of H• was more favorable than the formation of **2b**, assuming that the looseness of the loose TSs was similar. Even though several pathways were considered for the loss of H•, the loss of H_2 was still dominant in the dissociation of **1a** at low and moderate energies. However, at high energies, the loss of H• became dominant.

In the reported electron ionization (EI) spectrum of phenylarsane,[9] the relative abundances of the peaks at *m*/*z* 153, 152, 151, 79, and 78 were 14, 100, 33, 28, and 81, respectively. These peaks corresponded to the $[M\text{-}H]^+$, $[M\text{-}H_2]^{+\bullet}$, $[M\text{-}H_2\text{-}H]^+$, $[M\text{-}As]^+$, and $[M\text{-}AsH]^{+\bullet}$ ions, respectively. It is possible that the peak at *m*/*z* 151 peak was attributed to $[M\text{-}H\text{-}H_2]^+$, and the peak at 78 was caused by $[M\text{-}H\text{-}As]^+$ and/or $[M\text{-}As\text{-}H]^+$. The reported CID spectrum[9] of **1a** was similar to the EI spectrum. The greater loss of H_2 compared to H• suggests that the dissociations at low and moderate energies mainly contributed to the dissociations by the EI and the collision activation. However, the present theoretical prediction disagreed with the MID results. In the reported MID spectrum,[9] the loss of H• was predominant, and the H/D scrambling was not detected before the

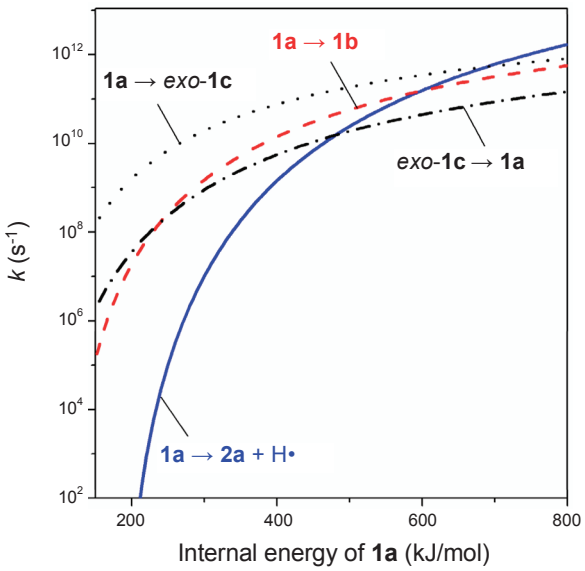

Figure 2. RRKM rate-energy dependence for the selected reaction steps in the primary dissociation of **1a**.

dissociation in the experiment for the $C_6H_5AsD_2^{+\bullet}$. The obtained RRKM rate-energy curves predicted that at low energies the loss of H_2 should be dominant and the H/D scrambling would occur before the dissociation, contrary to the MID results. In the QET, the dissociation was assumed to occur on the electronic ground state after the fast internal vibrational redistribution even when the reactant ion was generated in an electronic excited state. Recently, the existence of the long-lived electronic excited states of some polyatomic molecular ions was reported.[20-23] Some of the metastable **1a** ions in the electronic excited state possibly preferred the dissociation to **2a** + H• without the H scrambling, which was intensively detected in the MID experiment. Further experimental investigations are needed in order to examine this possibility.

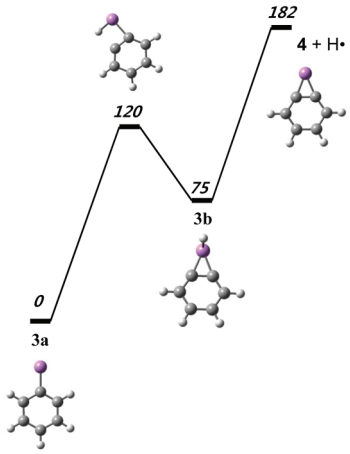

Figure 3. Potential energy diagram for the loss of H• from **3a**, which was derived from the G3//B3LYP calculations. The energies are presented in kJ mol^{-1}. The calculated total energy of **3a** was −2465.468705 hartrees.

Secondary dissociation. The further dissociations of $C_6H_5As^{+\bullet}$ and $C_6H_6As^+$ were investigated.

$$C_6H_5As^{+\bullet} \rightarrow C_6H_4As^+ + H\bullet \quad (6)$$

$$C_6H_6As^+ \rightarrow C_6H_5As^{+\bullet} + H\bullet \quad (7)$$

$$C_6H_6As^+ \rightarrow C_6H_4As^+ + H_2 \quad (8)$$

$$C_6H_6As^+ \rightarrow C_6H_6^{+\bullet} + As\bullet \quad (9)$$

Reaction 6 occurred through two consecutive steps (Figure 3). When the As of **3a** approached the ortho position, the ortho-H shifted to the As to form the benzoarsinidene radical cation (**3b**). Then the benzoarsininedenium ion (**4**) was formed through the direct As-H bond cleavage of **3b**. Alternatively, **4** was formed from **2a** (reaction 8) through the 1,3-H_2 elimination in two similar, consecutive steps in Figure 4. Comparing the overall energy barriers, **1a** → **3a** (+ H_2) → **4** + H• was energetically favored over **1a** → **2a** (+ H•) → **4** + H_2 by a value of 150 kJ mol^{-1} and, hence, was the main pathway in the formation of **4**.

The direct loss of H• from **2a** required a much higher energy

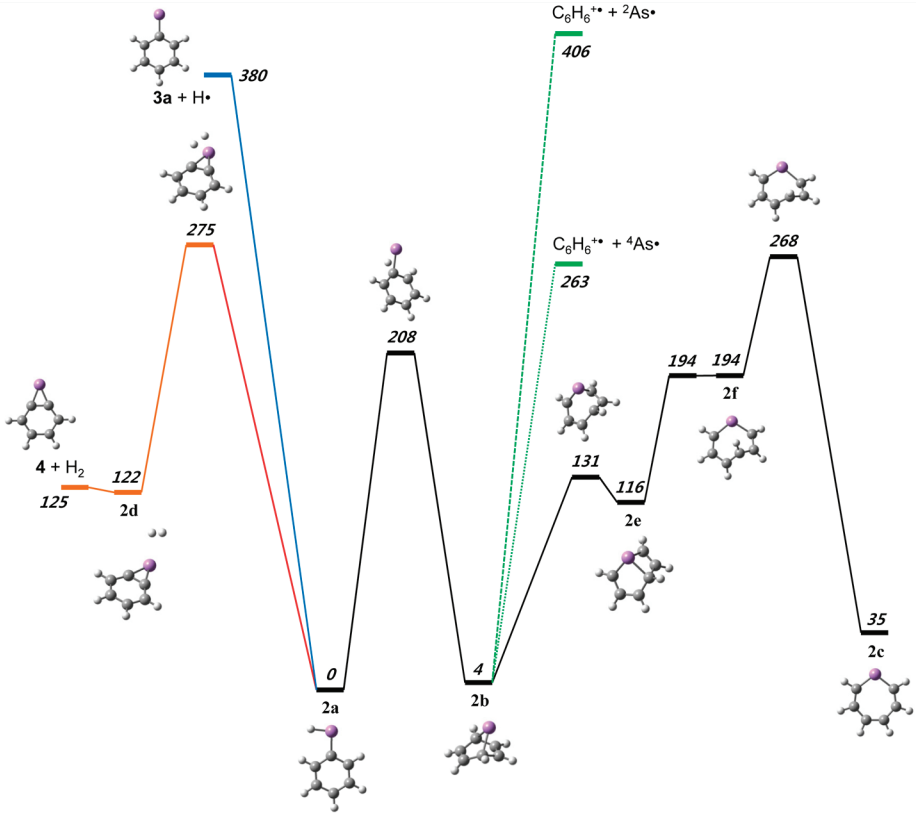

Figure 4. Potential energy diagram for the isomerization and the dissociation of **2a**, which was derived from the G3//B3LYP calculations. The energies are presented in kJ mol^{-1}. The calculated total energy of **2a** was -2466.115642 hartrees.

(380 kJ mol^{-1}) than the loss of H_2 (275 kJ mol^{-1}). The isomerization barrier between **2a** and **2b** was lower than the dissociation barriers. As• was removed from **2b** to form the benzene radical cation. The intersystem-crossing must occur from the singlet hypersurface in order to produce As• in a quartet state (^{4}As•). In the MID of **2a** that was generated from some phenylarsane derivatives, the loss of As• was the dominant reaction.[9] The additional intense peaks for the losses of H• and H_2 were detected in its CID,[9] indicating that the intersystem-crossing occurred near the products in the electronic ground states, $C_6H_6^{+\bullet} + {}^4$As•, after the fast isomerization of **2a** to **2b**. Alternatively, the benzene radical cation was produced through the loss of H• from the benzenium ion that was formed through the loss of As•.

2b isomerized to **2c** through ring expansion in three consecutive steps. The highest barrier in the isomerization pathway was comparable in energy to the loss of H_2 from **2a**. **2c** acted as a precursor for the losses of CH, C_2H_2, and C_4H_4 from **2a**, as observed in the CID experiment.[9]

Conclusions

The kinetic analysis based on the theoretical PES showed that the loss of H_2 from **1a** was favored over the loss of H• at low and moderate energies. These results explained the EI and CID spectra but not the MID spectrum, where the loss of H• was dominant. An isolated state could be involved in the MID. The consecutive reactions of **1a** → **3a** (+ H_2) → **4** + H• were the main pathway for the formation of **4**. The loss of As• occurred through the isomerization of **1a** to the bicyclic intermediate **1c**, which was more stable than **1a**. Considering the moderate abundance of the $[M\text{-}As]^+$ peak in the EI and CID spectra, the As atom that were produced must have been in the ground state (^{4}As•), as a result of the dissociation through the intersystem-crossing. The formation of $C_6H_6^{+\bullet} + {}^3$AsH from **1a** was thermodynamically favorable over the formation of $C_6H_6^{+\bullet} + {}^4$As• + H• through the consecutive reactions via **2b** because their overall endoergicities were 186 and 461 kJ mol^{-1}, respectively. Further studies on the intersystem-crossing points will be helpful for estimating their relative contributions to the formation of the benzene radical cation. The seven-membered ring intermediates did not play an important role in the dissociation of **1a**, unlike the aniline and phenylphosphine molecular ions because the losses of As• and AsH from the bicyclic isomer **1c** were more favored than the isomerization of **1c** to the seven-membered ring intermediates.

Acknowledgments. This work was supported by the National Research Foundation of Korea Grant funded by the Korean Government (2009-0072347).

Supplementary Information Available. Geometric structures for the selected species that were optimized using the B3LYP/6-31G(d) calculations are available.

References

1. Lifshitz, C. *Acc. Chem. Res.* **1994**, *27*, 138.
2. Lifshitz, C.; Gotkis, Y.; Ioffe, A.; Laskin, J.; Shaik, S. *Int. J. Mass Spectrom. Ion Processes* **1993**, *125*, 7.
3. Choe, J. C. *J. Phys. Chem. A* **2006**, *110*, 7655.
4. Choe, J. C.; Cheong, N. R.; Park, S. M. *Int. J. Mass Spectrom.* **2009**, *279*, 25.
5. Le, H. T.; Flammang, R.; Gerbaux, P.; Bouchoux, G.; Nguyen, M. T. *J. Phys. Chem. A* **2001**, *105*, 11582.
6. Choe, J. C. *Int. J. Mass Spectrom.* **2004**, *237*, 1.
7. Kim, S. Y.; Choe, J. C. *Int. J. Mass Spectrom.* **2010**, *294*, 40.
8. Kim, S. Y.; Choe, J. C. *Int. J. Mass Spectrom.* **2010**, *295*, 65.
9. Letzel, M.; Kirchhoff, D.; Grützmacher, H. F.; Stein, D.; Grützmacher, H. *Dalton Trans.* **2006**, 2008.
10. Letzel, M.; Grützmacher, H. F.; Stein, D.; Grützmacher, H. *Dalton Trans.* **2008**, 3282.
11. Choe, J. C. *Int. J. Mass Spectrom.* **2009**, *286*, 104.
12. Choe, J. C. *Bull. Korean Chem. Soc* **2007**, *28*, 319.
13. Choe, J. C. *Chem. Phys. Lett.* **2006**, *421*, 589.
14. Frisch, M. J.; Trucks, G. W.; Schlegel, H. B.; Scuseria, G. E.; Robb, M. A.; Cheeseman, J. R.; Scalmani, G.; Barone, V.; Mennucci, B.; Petersson, G. A.; Nakatsuji, H.; Li, X.; Hratchian, H. P.; Izmaylov, A. F.; Bloino, J.; Zheng, G.; Sonnenberg, J. L.; Hada, M.; Ehara, M.; Toyota, K.; Fukuda, R.; Hasegawa, J.; Ishida, M.; Nakajima, T.; Honda, Y.; Kitao, O.; Nakai, H.; Vreven, T.; Montgomery, J. A., Jr.; Peralta, J. E.; Ogliaro, F.; Bearpark, M.; Heyd, J. J.; Brothers, E.; Kudin, K. N.; Staroverov, V. N.; Kobayashi, R.; Normand, J.; Raghavachari, K.; Rendell, A.; Burant, J. C.; Iyengar, S. S.; Tomasi, J.; Cossi, M.; Rega, N.; Millam, J. M.; Klene, M.; Knox, J. E.; Cross, J. B.; Bakken, V.; Adamo, C.; Jaramillo, J.; Gomperts, R.; Stratmann, R. E.; Yazyev, O.; Austin, A. J.; Cammi, R.; Pomelli, C.; Ochterski, J. W.; Martin, R. L.; Morokuma, K.; Zakrzewski, V. G.; Voth, G. A.; Salvador, P.; Dannenberg, J. J.; Dapprich, S.; Daniels, A. D.; Farkas, Ö.; Foresman, J. B.; Ortiz, J. V.; Cioslowski, J.; Fox, D. J. Gaussian 09, Revision A. 02, Gaussian. In *Inc., Wallingford CT*, 2009.
15. Baboul, A. G.; Curtiss, L. A.; Redfern, P. C. *J. Chem. Phys.* **1999**, *110*, 7650.
16. Baer, T.; Hase, W. L. *Unimolecular Reaction Dynamics: Theory and Experiments*; Oxford University Press: New York, 1996.
17. Beyer, T.; Swinehart, D. R. *ACM Commun.* **1973**, *16*, 379.
18. Scott, A. P.; Radom, L. *J. Phys. Chem. A* **1996**, *100*, 16502.
19. Lifshitz, C. *Adv. Mass Spectrom.* **1989**, *11*, 713.
20. Kim, M. S.; Kwon, C. H.; Choe, J. C. *J. Chem. Phys.* **2000**, *113*, 9532.
21. Youn, Y. Y.; Kwon, C. H.; Choe, J. C.; Kim, M. S. *J. Chem. Phys.* **2002**, *117*, 2538.
22. Youn, Y. Y.; Choe, J. C.; Kim, M. S. *J. Am. Soc. Mass Spectrom.* **2003**, *14*, 110.
23. Kwon, C. H.; Kim, M. S.; Choe, J. C. *J. Am. Soc. Mass Spectrom.* **2001**, *12*, 1120.